

SUPPLEMENTAL INFORMATION

SUPPLEMENTAL MATERIALS AND METHODS

Analysis of global changes in protein expression upon HLX1 knockdown. To evaluate the changes in protein levels caused by knockdown of HLX1, we took advantage of SILAC, which allows for quantitative mass spectrometry comparisons between complex samples. To this end, IMR-90 cells at passage 12 were infected with pRS or pRS-shHLX1.2 retroviruses and one day after infection, cells were grown in cell culture media with 'Light' (L, pRS-shHLX1.2 infected cells) or 'Heavy' (H, pRS-infected cells) isotope containing amino acids. 3 days after switching to H or L medium, cells were selected with puromycin for 4 additional days and cell pellets collected for analysis 6 days after selection. Specifically, for the 'Heavy' sample, IMR-90 cells were grown in Heavy SILAC DMEM (Pierce), supplemented with 10 % dialyzed FBS (Biosera, East Sussex, UK), containing $^{13}\text{C}(6)^{15}\text{N}(2)$ labeled lysine and $^{13}\text{C}(6)^{15}\text{N}(4)$ labeled arginine (CK gas, Hampshire, UK). Cell pellets were lysed using RIPA buffer and protein extracts subjected to SDS-PAGE. In total, 19 gel pieces were subjected to overnight in-gel trypsin digestion. The peptide extracts were subjected to a second round of trypsin digestion to minimize the number of missed cleavages. Peptide mixtures were analyzed using an UltiMate 3000 Rapid Separation LC, coupled to a LTQ-Orbitrap-Velos mass spectrometer (ThermoFisher Scientific). Separation was performed in a 3 h gradient using a 50 cm Acclaim pepmap c18 column. Protein identification and quantification was performed using Maxquant v1.2.0.13, with the embedded Andromeda 1.2.0.0 search engine and the IPI_Human_v3.37 database. The initial minimum ratio H/L count was set to 1, but to generate the data presented in Fig 3A and Table S1, the stringency was increased to a minimum ratio H/L count of 3 and a minimum unique peptide count of 2 per protein group. Note that Fig 3A and Table S1 show the log of the intensity of the ratio between the shHLX1.2 cells and the control pRS-infected cells (therefore the L/H ratio).

High Content Analysis. High Content Analysis (HCA) was performed as described elsewhere (Banito et al, 2009; Barradas et al, 2009; Bishop et al, 2010). Briefly, cells were seeded in 96-

well plates (Nunc) and visualized by IF. Two fluorescence images corresponding to DAPI and primary antibody/Alexa Fluor 488-secondary antibody were acquired for each field using the IN Cell Analyzer 1000 automated epifluorescence microscope at 10x magnification (GE Healthcare). HCA was performed using the IN Cell Investigator software (v1.7; GE Healthcare). For the analysis, DAPI staining of the nuclei was used to identify cells. The nuclei were then segmented using top-hat segmentation, specifying a minimum nucleus area of 100 μm^2 . To define the cell segmentation, a collar segmentation routine was used with a ratio of 1 μm . To determine the cellular expression of the analyzed protein, the average intensity of pixels in the reference channel (Alexa Fluor 488) within the specified nuclear region (Object Nuclear Intensity) was measured. Each cell was assigned a nuclear intensity value for the specific protein expression and that value was used to set up a threshold filter, which determined positive and negative expressing cells. The threshold filter used a histogram for data visualization. In order to set the filter cut-off, expression in control cells was measured to define the negative population, followed by the analysis of the positive control. Once the cut-off was set up, analysis of the experiment was carried out. As a result, the software classified each cell as either positive or negative for the expression of the analyzed protein. The mean of the nuclear intensity was also routinely analyzed and equivalent results were obtained. The antibodies used for the analysis were tested with adequate controls (shRNAs or siRNAs) to test their specificity and if possible, alternative antibodies were tested in control experiments to confirm the results obtained.

Analysis of homeodomain DNA-binding similarity. Correlations between Homeobox DNA binding profiles were performed, as described in (Berger et al, 2008). Assessment of the significance of correlation within the 7 genes that we identified in Fig 8A as able to prevent the induction of the *INK4a* promoter (DLX3, HOXA9, HOXB13, HOXC13, HOXD3 and HOXD8 in addition to HLX1) was performed by comparing the correlation within these 7 genes to that within 1,000,000 random Homeobox gene sets of equal size. Significance was therefore

calculated empirically, as the proportion of random gene sets having higher mean correlation than the set under investigation.

SUPPLEMENTAL REFERENCES

Ben-Porath I, Thomson MW, Carey VJ, Ge R, Bell GW, Regev A, Weinberg RA (2008) An embryonic stem cell-like gene expression signature in poorly differentiated aggressive human tumors. *Nat Genet* **40**: 499-507

Berger MF, Badis G, Gehrke AR, Talukder S, Philippakis AA, Pena-Castillo L, Alleyne TM, Mnaimneh S, Botvinnik OB, Chan ET, Khalid F, Zhang W, Newburger D, Jaeger SA, Morris QD, Bulyk ML, Hughes TR (2008) Variation in homeodomain DNA binding revealed by high-resolution analysis of sequence preferences. *Cell* **133**: 1266-1276

Bishop CL, Bergin AM, Fessart D, Borgdorff V, Hatzimasoura E, Garbe JC, Stampfer MR, Koh J, Beach DH (2010) Primary cilium-dependent and -independent Hedgehog signaling inhibits p16(INK4A). *Mol Cell* **40**: 533-547

Nuytten M, Beke L, Van Eynde A, Ceulemans H, Beullens M, Van Hummelen P, Fuks F, Bollen M (2008) The transcriptional repressor NIPP1 is an essential player in EZH2-mediated gene silencing. *Oncogene* **27**: 1449-1460

Senese S, Zaragoza K, Minardi S, Muradore I, Ronzoni S, Passafaro A, Bernard L, Draetta GF, Alcalay M, Seiser C, Chiocca S (2007) Role for histone deacetylase 1 in human tumor cell proliferation. *Molecular and cellular biology* **27**: 4784-4795

SUPPLEMENTAL TABLES

Supplemental Table S1. Global changes in protein levels upon HLX1 knockdown analyzed by SILAC.

This table is included as an independent Excel file (SupplementalTableS1.xlsx).

Supplemental Table S2. Details of siRNAs used in this study.

This table is included in this document (page 11).

Supplemental Table S3. Details of oligonucleotide primers and TaqMan probes used in this study.

This table is included in this document (page 12).

Supplemental Table S4. Oligonucleotides used for DNA precipitation assays.

This table is included in this document (page 13).

SUPPLEMENTAL FIGURE LEGENDS**Sup Fig S1. A screen for transcription regulators extending cellular lifespan identifies the Homeobox protein HLX1.**

(A, B) We cloned the indicated genes (HEY1, MSX2, NAB2, HLX1, SPDEF, TGIF and TSC22D4) into retroviral vectors and infected IMR-90 cells (passage 17) with either these vectors or appropriate controls (vector, hTERT or shp53). IMR-90 cells were then subjected to serial passage and the effect on cell growth analyzed by colony formation assays and crystal violet staining (A) or by plotting growth curves (B). The colony formation assay shown in (A) corresponds to passage 24. (C) WI-38 human fibroblasts were infected with the indicated retroviral vectors and growth curves were performed after selection.

Sup Fig S2. Expression of point mutants of the HLX1 homeodomain causes premature senescence.

(A) Cartoon depicting the domain structure of HLX1 (left). Domains were identified using Ensembl. Marked in color are a Glutamine-rich region (Gln), the Homeobox DNA-binding domain (homeodomain, Homeo) and a Serine-rich region (Ser). The two conserved residues in the homeodomain (A322 and T328) targeted to generate the mutants are highlighted. HLX1 wt and the homeodomain point mutants (A322T and T328M) are expressed to comparable levels, as shown by IB (right). (B) IMR-90 cells (passage 17) were infected with retroviral vectors expressing HLX1 wt, A322T, T328M or the indicated controls and growth curves were performed after selection. (C, D). At the time point indicated by an arrow in panel B, cells were seeded to perform p16^{INK4a} IF. The percentage of p16^{INK4a} positive cells is shown in (C) and representative images are shown in (D). Analysis was performed at passage 24.

Sup Fig S3. Knockdown of HLX1 using retroviral or lentiviral-mediated shRNA delivery.

(A) Cartoon depicting the human HLX1 mRNA (accession number NM_021958.3), summarizing the positions targeted by the different shRNAs and siRNAs used in this study. Sequences targeted by the 4 siRNAs and shRNAs are different. (B) IMR-90 cells were infected with a

lentiviral control vector (pLKO) or a lentiviral vector targeting HLX1 (pLKO-shHLX1.2). The efficiency of the knockdown achieved by the pLKO-shHLX1.2 vector in IMR-90 cells was assessed by IB (left) and qRT-PCR (second from left). The numbers under the blots correspond to quantification of HLX1 signal normalized to α -tubulin. The effect of knocking down HLX1 on BrdU incorporation was measured using IF (second from right). HLX1 effect on INK4a transcription was monitored by qRT-PCR (right). (C) IMR-90 cells were infected with retroviral shRNA vectors targeting HLX1 or p16^{INK4a} and subjected to p16^{INK4a} IF after selection. Representative images (left) and a quantification of the percentage of p16^{INK4a} positive cells (right) are presented (passage 14).

Sup Fig S4. HLX1 knockdown by siRNA transfection causes growth arrest and induces p16^{INK4a}.

(A) HPrEC, NHK or IMR-90 cells were transfected with the indicated siRNAs and 5 days later, the number of cells was counted in an equal number of fields using HCA software. (B, C) HPrEC, NHK or IMR-90 cells were transfected with the indicated siRNAs and 5 days later subjected to p16^{INK4a} IF. Representative images are presented in (B) and the percentage of p16^{INK4a} positive cells is presented in (C).

Sup Fig S5. HLX1 expression represses p16^{INK4a}, but does not affect the levels of p53 or p21^{CIP1} in IMR-90 cells.

Representative images of DAPI (top) and either p53 (A), p21^{CIP1} (B) or p16^{INK4a} (C) IF (bottom) in IMR-90 cells infected with the indicated vectors. The images correspond to the data presented in Fig 3C.

Sup Fig S6. E7 rescues the growth arrest caused by HLX1 depletion.

IMR-90 cells were infected with a control retrovirus (vector) or a retrovirus expressing the oncoviral protein E7, which targets RB and other pocket proteins for degradation. IF against RB was conducted (left) and quantification shows the effect of E7 expression over RB levels (centre). Expression of E7 significantly prevents the arrest caused by HLX1 depletion as measured by BrdU incorporation (right).

Sup Fig S7. HLX1 regulates PRC target genes.

(A, B) GSEA of gene sets associated with HDAC targets (Senese et al, 2007) and PRC2 targets (Ben-Porath et al, 2008) are found enriched in transcriptional profiles of IMR-90 cells in which HLX1 expression has been knocked down. (C, D) Additional gene sets extracted from the Ben Porath et al. and Bracken et al. studies (Ben-Porath et al, 2008; Bracken et al, 2006) are enriched in transcriptional profiles of IMR-90 cells in which HLX1 expression has been knocked down. (E) GSEA of gene sets associated with HDAC targets (Senese et al, 2007) and EZH2 targets (Nuytten et al, 2008) were found enriched in transcriptional profiles of URE mouse leukemic cells in which HLX1 expression was knocked down (Kawahara et al, 2012). (F) Enrichment for PRC2 targets gene sets in transcriptional profiles of IMR-90 cells in which CBX7 expression has been knocked down. NES, normalized enrichment score; FDR, false discovery rate.

Sup Fig S8. *In situ* PLA shows that HLX1 is associated with HDAC1 and the PRC2 complex.

(A) *In situ* PLA in HEK 293T cells transfected with HLX1 and FLAG-SUZ12 or HLX1 and FLAG-HDAC1. Antibodies against FLAG and HLX1 were used to detect the protein complexes. (B) *In situ* PLA in IMR-90 cells infected with FLAG-HLX1. Antibodies against FLAG and rabbit antibodies recognizing HDAC1, SUZ12 or RING1A were used to detect the protein complexes. (C) *In situ* PLA in IMR-90 cells infected with the indicated lentiviruses. Antibodies against HDAC1 and HLX1 were used to detect the protein complexes. Representative images (left) and a quantification of the percentage of cells displaying an interaction (right) are shown. Cells presenting 10 or more nuclear spots were scored as positive. F, FLAG; H, HLX1; F+H, FLAG and HLX1. Blue: DAPI; Red: PLA signal.

Sup Fig S9. HLX1 does not immunoprecipitate with PRC1 components.

HEK 293T cells were transfected with plasmids expressing HLX1 and a FLAG-tagged version of BMI1, RING1A or HPH2 as indicated. Total lysates or FLAG immunoprecipitates were prepared and immunoblots conducted using antibodies recognizing HLX1 or the FLAG epitope. Specific

bands are indicated with an arrow, while non-specific bands are denoted by *. WB, western blot; IP, immunoprecipitation. These experiments were performed simultaneously with the experiments presented in Fig 6B-C which show an interaction between HLX1 and PRC2 components and between HLX1 and HDAC1.

Sup Fig S10. SUZ12 and HDAC1 mediate the regulation of p16^{INK4a} by HLX1.

(A, B) IF showing the effects of siRNAs targeting SUZ12 and HDAC1 corresponding to those used in the experiment presented in Fig 7A-C. (C) Representative p16^{INK4a} IF pictures corresponding to the data presented in Fig 7C.

Sup Fig S11. CBX7 depletion results in reduced PRC occupancy of the *INK4a* promoter.

(A) IMR-90 cells (passage 12-13) were infected with a control lentiviral vector (pLKO) or a vector knocking down CBX7 (pLKO-shCBX7.5) and CBX7 and *INK4a* mRNA levels were analyzed by qRT-PCR. (B) ChIP analysis showing the effect of CBX7 depletion on occupancy of the *INK4a* promoter (primer set 6). Occupancy of the *INK4a* promoter by CBX7, RING1B, SUZ12 and levels of H3K27me3 were analyzed at passage 14-15.

Sup Fig S12. HLX1^{T328M} mutant fails to recruit PRC to the *INK4a* locus.

(A, B) The mutant and wt versions of HLX1 co-immunoprecipitate with SUZ12 (A) and HDAC1 (B). HEK 293T cells were transfected with plasmids expressing HLX1 and a FLAG-tagged version of SUZ12 (A) or HDAC1 (B) as indicated. Total lysates or FLAG immunoprecipitates were prepared and immunoblots conducted using antibodies recognizing HLX1 or the FLAG epitope. Specific bands are noted by an arrow and IgG bands by an asterisk. WB, western blot; IP, immunoprecipitation. (C) DNA pulldown assays showing the reduced binding of HLX1 T328M to a probe corresponding to the ~ -550 position. (D, E) IMR-90 cells were infected at passage 17 with an empty vector (vector) or retroviruses expressing HLX1 wt or HLX1 T328M. Their effect over p16^{INK4a} expression was measured by qRT-PCR (D). (E) ChIP analysis showing the effect of HLX1 wt and HLX1 T328M on occupancy of the *INK4a* promoter (primer

set 6). The occupancy of the locus by HLX1, RING1B, SUZ12 and levels of H3K27me3 was analyzed at passage 24.

Sup Fig S13. Knockdown of selected homeodomain-containing proteins in HPrEC.

(A) HPrEC were transfected with the indicated siRNAs and 5 days later, cells were collected, RNA prepared and the levels of the specific target genes (listed at the top of the graph) measured by qRT-PCR. The graph shows the relative mRNA expression compared with scrambled siRNA transfected cells. (B) HPrEC were transfected with the indicated siRNAs and cell numbers determined 5 days later using HCA software. As a reference, a gray background represents the cell number in HPrEC transfected with scrambled control siRNAs. (C) Plot denoting the correlation between 10^6 random combinations of 7 homeodomain-containing proteins, as described in (Berger et al, 2008). A red line marks the correlation between the 7 homeodomain-containing proteins that we identified as p16^{INK4a} regulators (HLX1, DLX3, HOXA9, HOXB13, HOXC13, HOXD3 and HOXD8). Correlation was 0.82, $p=0.038$.

Sup Fig S14. HOXA9 expression regulates senescence via PRC2- and HDAC1-dependent INK4a repression.

(A) HOXA9 expression in IMR-90 cells extends cellular lifespan. Crystal violet staining of IMR-90 cells infected with a control vector or expressing HOXA9. (B) *In situ* PLA in IMR-90 cells infected with FLAG-HOXA9. Antibodies against FLAG and the indicated proteins were used to detect the protein complexes. Cells presenting 10 or more nuclear spots were scored as positive. The percentage of cells displaying an interaction is shown. (C) HEK 293T cells were transfected with a vector expressing a FLAG-tagged version of HOXA9, as indicated. Total lysates, FLAG or HA immunoprecipitates were prepared and immunoblots conducted using FLAG or HDAC1 antibodies. WB, western blot; IP, immunoprecipitation.

Sup Fig S15. Relation between HLX1 and HOXA9 on p16^{INK4a} regulation.

(A) IMR-90 cells were infected at passage 15 with a control retrovirus (vector) or retroviruses expressing HOXA9 (HOXA9). The effect of knocking down HLX1 expression over p16^{INK4a} levels was measured using quantitative IF at passage 24-27 (left). IMR-90 cells were infected with a

control retrovirus (vector) or retroviruses expressing HLX1 (HLX1). The effect of knocking down HOXA9 expression over p16^{INK4a} levels was measured using quantitative IF (right). Average of the nuclear intensity of p16^{INK4a} is shown. a.u, arbitrary units. (B, C) HLX1 interacts with HOXA9. (B) HEK 293T cells were transfected with plasmids expressing HLX1 and a FLAG-tagged version of HOXA9. Total lysates or FLAG immunoprecipitates were prepared and immunoblots conducted using antibodies recognizing HLX1 or the FLAG epitope. WB, western blot; IP, immunoprecipitation. (C) *In situ* PLA in IMR-90 cells. Antibodies against HOXA9 and the indicated proteins were used to detect the protein complexes. Cells presenting 10 or more nuclear spots were scored as positive. The percentage of cells displaying an interaction is shown.

Sup Fig S16. Expression of HLX1 and other Homeobox genes tested does not decrease during senescence.

(A) qRT-PCR analysis showing the expression of *HLX1* and *INK4a* during serial passage of IMR-90 (replicative senescence) and upon treatment with 100 nM 4OHT of IMR-90 ER:RAS cells (OIS). (B) The expression of the six Homeobox genes tested does not change or increases during replicative senescence. (C) qRT-PCR analysis of the levels of PRC2 components (EZH2, EED and SUZ12) during replicative senescence and OIS.

Supplemental Table S2. Details of siRNAs used in this study.

Targeted gene	siRNA	Catalogue no.	Target sequence
PPIB	siGLO	D-001630-02-05	GGAAAGACTGTTCCAAAAA
-	AllStars	SI03650318	<i>not provided</i>
GFP	Ctrl_GFP_2	SI04380467	AAGCAGCACGACTTCTTCAAG
CBX7	Hs_CBX7_7	SI04155312	CGCCGTGGAGAGCATCCGGAA
INK4a	Hs_CDKN2A_15	SI02664403	TACCGTAAATGTCCATTTATA
	Hs_SUZ12_5	SI03132885	AAGGATGTAAGTTGTCCAATA
SUZ12	Hs_SUZ12_6	SI03246817	TAGCATAATGTCAATAGATAA
	Hs_SUZ12_7	SI04156537	AAGGATATTTGTATCAGGGTT
	Hs_HDAC1_3	SI00070623	CCACAGCGATGACTACATTAA
HDAC1	Hs_HDAC1_4	SI00070630	CGGGATTGATGACGAGTCCTA
	Hs_HDAC1_6	SI02663472	CACCCGGAGGAAAGTCTGTTA
	Hs_DLX3_6	SI03073063	CAGTGATTCCATGGCCTGCAA
DLX3	Hs_DLX3_7	SI03090745	CTCCTGGTATCACGCACAGAA
	Hs_HLX_2	SI00439299	AAGGTTTGAGATTCAGAAGTA
HLX1	Hs_HLX_5	SI03228169	TAGGACGCCTTAAATTTGTAA
	Hs_HOXA9_6	SI04239165	CTACCTAGGGTTTATGCTTAA
HOXA9	Hs_HOXA9_8	SI04346370	CCCATCGATCCAATAACCCA
	Hs_HOXB13_5	SI04133304	TCCGGGATATCCGGGAACCTA
HOXB13	Hs_HOXB13_7	SI04367902	CTCCATGGAGCCCGGCAATTA
	Hs_HOXC13_4	SI00117971	CAGGAGCGAGGTGTCTCCCTA
HOXC13	Hs_HOXC13_5	SI03098011	CTGGCCGGAGAGCCTTATGTA
	Hs_HOXD3_6	SI04209520	CTCGCCATAAATCAGCCGCAA
HOXD3	Hs_HOXD3_8	SI04315318	AAGAGTCTCGACAGAACTCCA
	Hs_HOXD8_5	SI04258709	AGCCGAAGGCCTGACAAATTA
HOXD8	Hs_HOXD8_6	SI04286387	AGAGGCCGAGCTGGTACAATA

Supplemental Table S3. Details of oligonucleotide primers and TaqMan probes used in this study.**Primers used for qRT-PCR**

Target	Forward primer	Reverse primer
Human ANKRD1	GGCCACTATGAGTGCGCGGAG	TCCATCGGCGTCTTCCCAGC
Human AREG	GCGAAGGACCAATGAGAGCCCC	TGGTCCCCAGAAAATGGTTCACGC
Human BMP2	GGACATTCGGTCTTGCGCCA	GGTCGACCTTTAGGAGACCGC
Human CLDN1	GGCTGTCATTGGGGGTGCGATA	GGCAGAGAGAAGCAGCAGCCC
Human CTSS	AGTTCCCTGAGAGTTCCCAGCC	GGCCCCCACAGCACTGAAAG
Human CYP1B1	ACTGACATCTTCGGCGCCAGC	CAAGGCAGACGGTCCCCTCCC
Human FER1L6	GTGGTTCATGAGCCCCTTTA	CTATGAGCCCACAACGATCC
Human GDF15	GGATACTCACGCCAGAAGTGC	AGGGCGGCCCGAGAGATACG
Human IL8	GAGTGGACCACACTGCGCCA	TCCACAACCCTCTGCACCCAG
Human INK4A	CGGTCCGAGGCCGATCCAG	GCGCCGTGGAGCAGCAGCAGCT
Human KYNU	TGGGAGCCAAACACTCCATTGGG	CGCAATGCGCTGCACTGTGT
Human PAPPA	CTGGCTGAACCCACACGGG	GGAGGTGCAGCAATCCCCACC
Human PRDMI	GGTACACACGGGAGAAAAGC	GCAGTTTCAGGTGCACAAAC
Human RPS14	TCACCGCCCTACACATCAAAC	CTGCGAGTGCTGTGAGAGG
Human SSP1	GGACATCACCTCACACATGG	GTGGGTTTCAGCACTCTGGT
Human UIMC1	GCTTCTCCAGATGCCGGGGCT	CACATCCTTCTTCTCCAGTTCCGA

TaqMan probes used for qRT-PCR

Target	Probe
Human GAPDH	4333764F
Human TBP	4333769F
Human CBX7	Hs00545603_m1
Human DLX3	Hs00270938_m1
Human EZH2	Hs01016789_m1
Human EED	Hs00537777_m1
Human HLX1	Hs00172035_m1
Human HOXA9	Hs00365956_m1
Human HOXB13	Hs00197189_m1
Human HOXC13	Hs00600868_m1
Human HOXD3	Hs00232506_m1
Human HOXD8	Hs00251905_m1
Human SUZ12	Hs00248742_m1

Primers used for ChIP

Primers	Relative Location	Forward primer	Reverse primer
PS1	<i>INK4b</i> , exon 1	GGAACCTAGATCGCCGATGTAG	TGTTTTACGCGTGGAATGCAC
PS2	<i>ARF</i> , exon 1	GTGGGTCCCAGTCTGCAGTTA	CCTTTGGCACCAGAGGTGAG
PS3	4.5 kb downstream <i>ARF</i> start site	GGAGCGATGTGATCCGTTATC	TGAAATCCCAATCGTCTTCCAC
PS4	15 kb downstream <i>ARF</i> start site	GCACTTGCCCTTCCAGGTATA	TGATAGTTCAAGGCCCTATGCC
PS5	1 kb upstream <i>INK4a</i> promoter	CTCAAAGCGGATAAATCAAGAGC	AAGCCTTAAGAACAGTGCCACAC
PS6	0.2 kb upstream <i>INK4a</i> promoter	ACCCCGATTCAATTTGGCAG	AAAAAGAAATCCGCCCCCG
PS7	3' end <i>INK4a</i> , exon 1	AGAGGGTCTGCAGCGG	TCGAAGCGCTACCTGATTCC
PS8	0.2 kb downstream <i>INK4a</i> , exon 1	GCCAAGGAAGAGGAATGAGGAG	CCTTCAGATCTTCTCAGCATTCCG
PS12	9.0 kb downstream <i>INK4a</i> , exon 1	ACAGGGCGGCTCAAACAATAG	ATGTAAGGACACAGTGGGAAGGGG
<i>CCND1</i>	0.1 kb downstream <i>CCND1</i> promoter	CACGGACTACAGGGGAGTTTTG	TTCCACTTCGCAGCACAGGAG

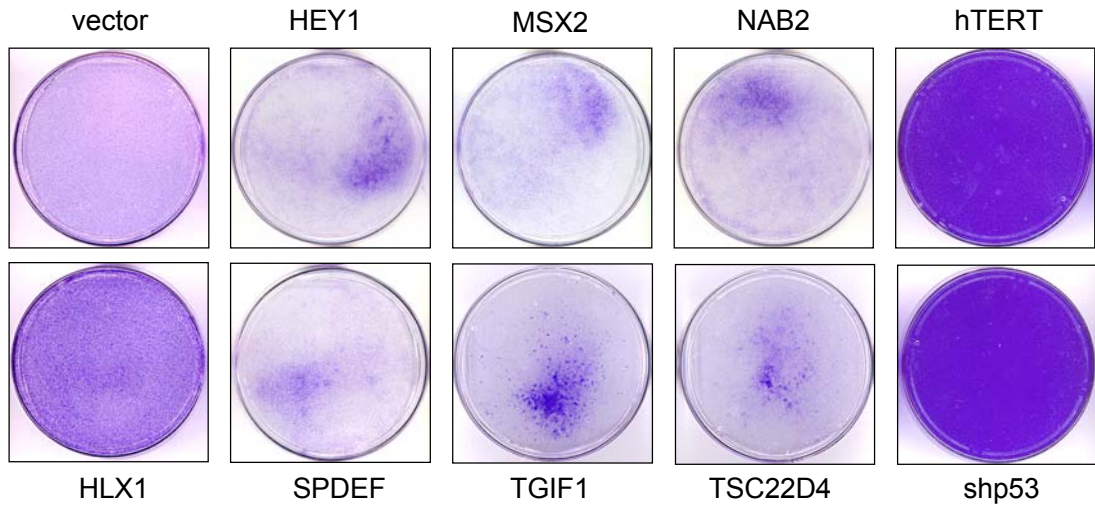
Supplemental Table S4. Oligonucleotides used for DNA pulldown assays.

Probe	Forward oligonucleotide	Reverse oligonucleotide
A	GGTATTAGCTTAGGATGTGTGGCACTGTTCTTAAGGCTTA	TAAGCCTTAAGAACAGTGCCACACATCCTAAGCTAATACC
B	GCACTGTTCTTAAGGCTTATATGT ATTA AATACATCATTTA	TAAATGATGTATTAATACATATAAGCCTTAAGAACAGTGC
B.m1	GCACTGTTCTTAAGGCGGGGGTGT ATTA AATACATCATTTA	TAAATGATGTATTAATACACCCCGCCTTAAGAACAGTGC
B.m2	GCACTGTTCTTAAGGCTTATATGTATGGGGGCATCATTTA	TAAATGATGCCCCCATACATATAAGCCTTAAGAACAGTGC
C	TATGT ATTA AATACATCATTTAAACTCACAAACAACCCCTAT	ATAGGGGTTGTTGTGAGTTTAAATGATG ATTA AATACATA
C.m	TATGTATGGGGCATCATTTAAACTCACAAACAACCCCTAT	ATAGGGGTTGTTGTGAGTTTAAATGATGCCCCCATACATA
D	AACTCACAAACAACCCCTATAAAGCAGGGGGCACTCATATT	AATATGAGTGCCCCCTGCTTTATAGGGGTTGTTGTGAGTT
E	AGTCCGTCCTTCCAATGACTCCCTCCCATTTCCTATCT	AGATAGGAAAATGGGGAGGGAGTCATTGGAAGGACGGACT
F	CCCTCCCATTTCCTATCTGCCTACAGGCAGAATTCTCC	GGAGAATTCTGCCTGTAGGCAGATAGGAAAATGGGGAGGG
G	GCCTACAGGCAGAATTCTCCCCGTCGG ATTA AATAAAC	GTTTATTT ATA ACGGACGGGGGAGAATTCTGCCTGTAGGC
G.m	GCCTACAGGCAGAATTCTCCCCGTCGGGGGG AATAAAC	GTTTATTTCCCGCGGACGGGGGAGAATTCTGCCTGTAGGC
H	CCCGTCGG ATTA AATAAACCTCATCTTTTCAGAGTCTGC	GCAGACTCTGAAAAGATGAGGTTTATTT ATA ACGGACGGG
H.m	CCCGTCGGGG AATAAAC CTCATCTTTTCAGAGTCTGC	GCAGACTCTGAAAAGATGAGGTTTATTTCCCGCGGACGGG
I	CTCATCTTTTCAGAGTCTGCTTTATACCAGGCAATGTAC	GTACATTGCCTGGTATAAGAGCAGACTCTGAAAAGATGAG

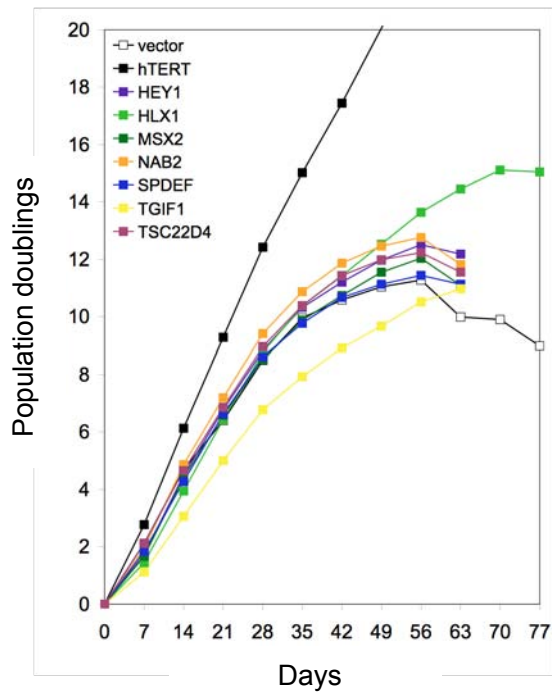
Underlined: mutated sequences

Bold: core ATTA Homeobox-binding motif on the forward oligo.

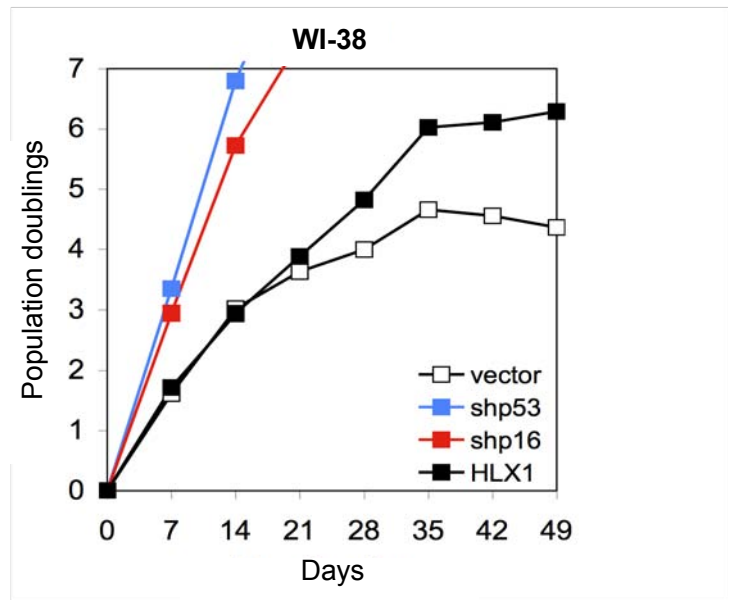
A



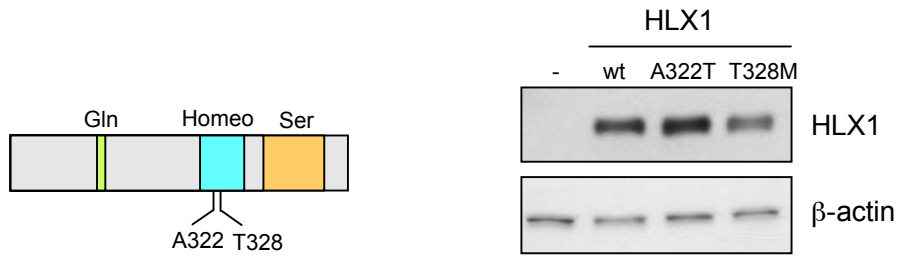
B



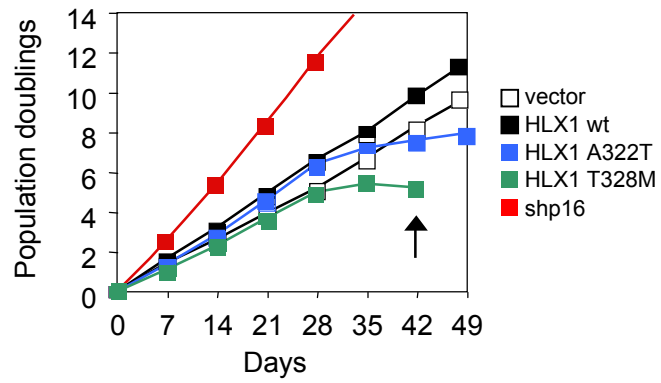
C



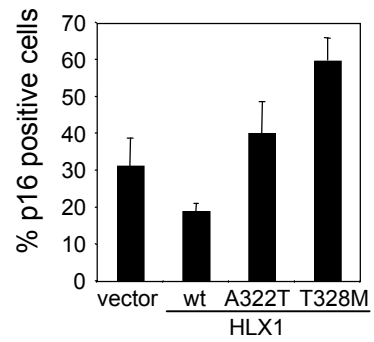
A



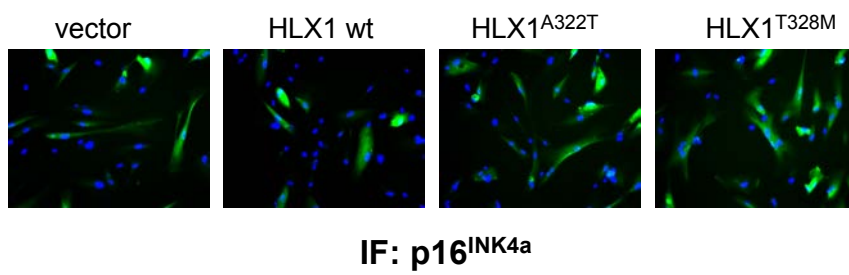
B

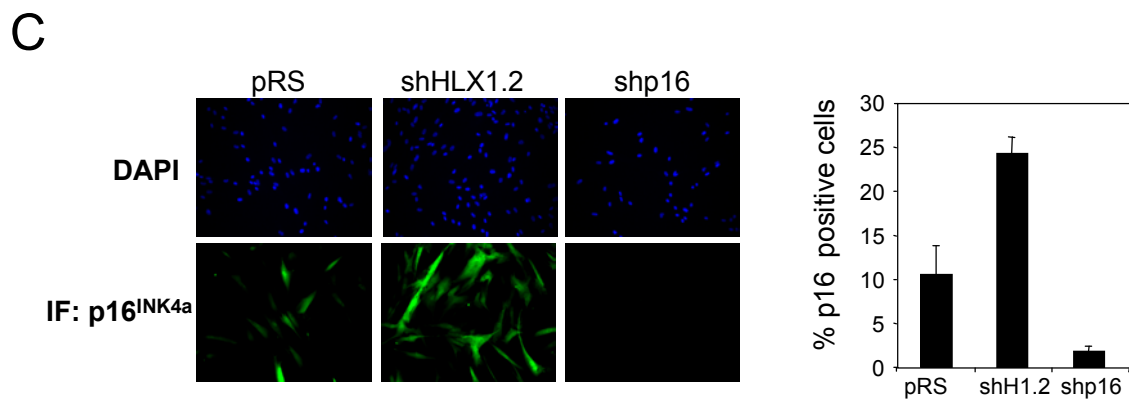
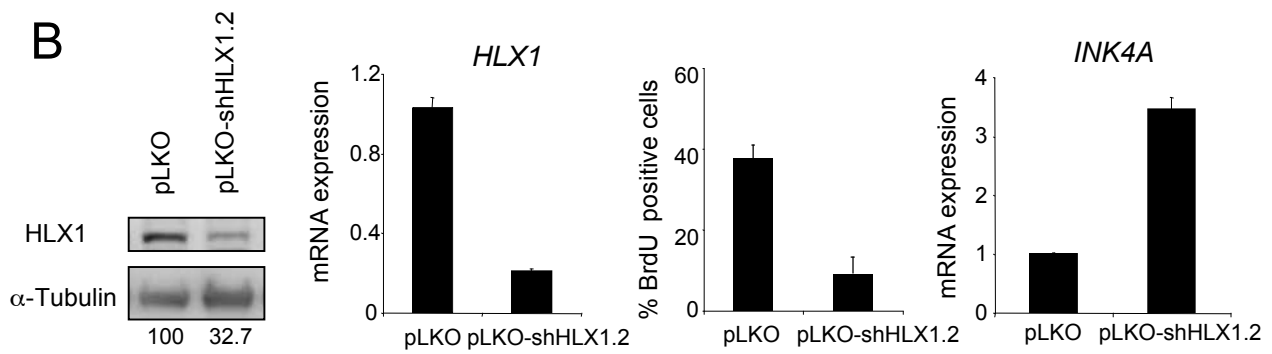
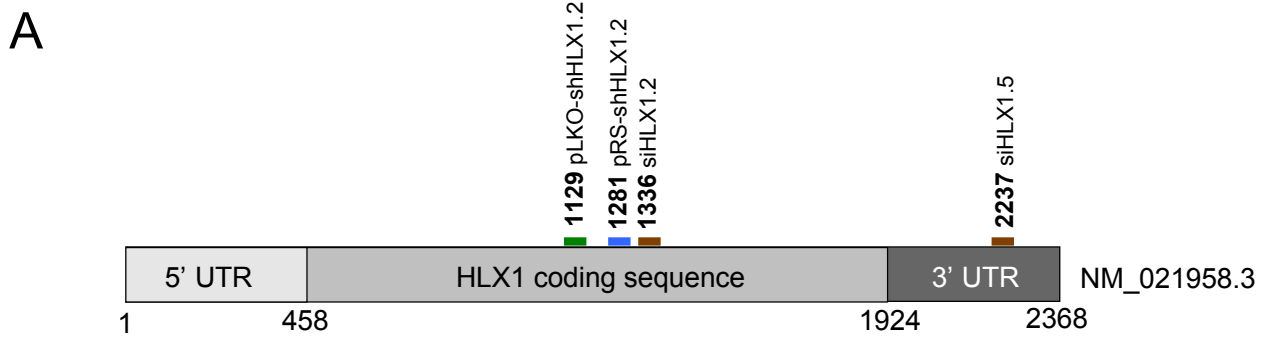


C

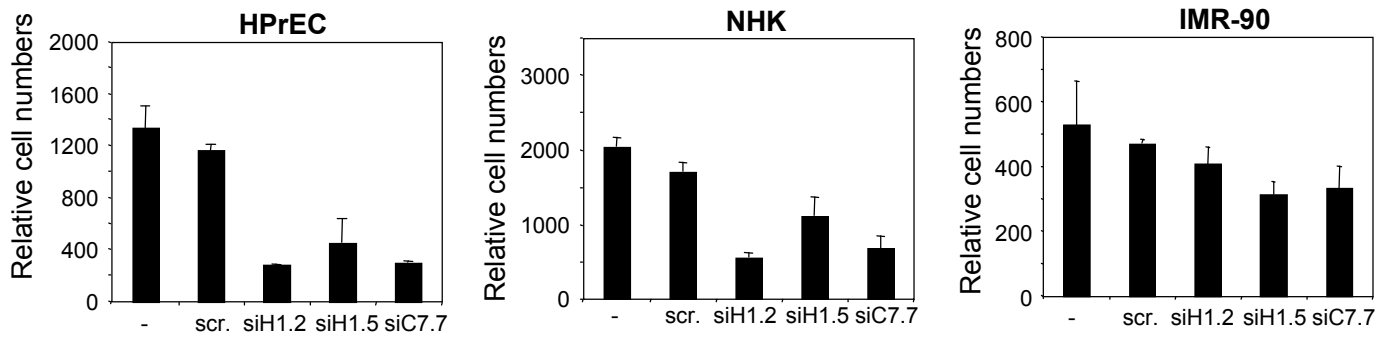


D

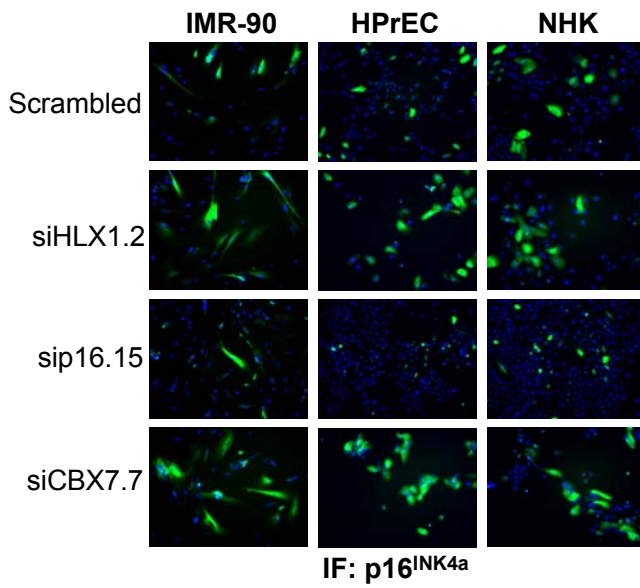




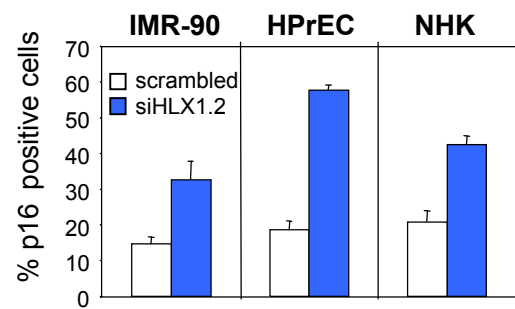
A



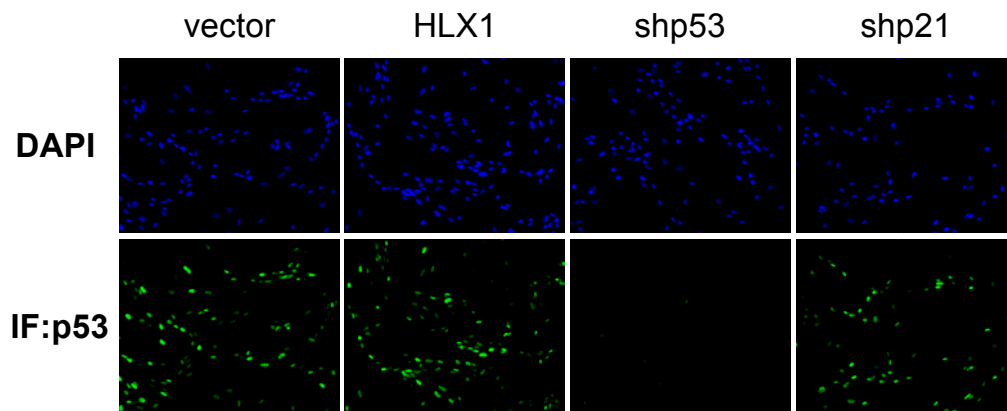
B



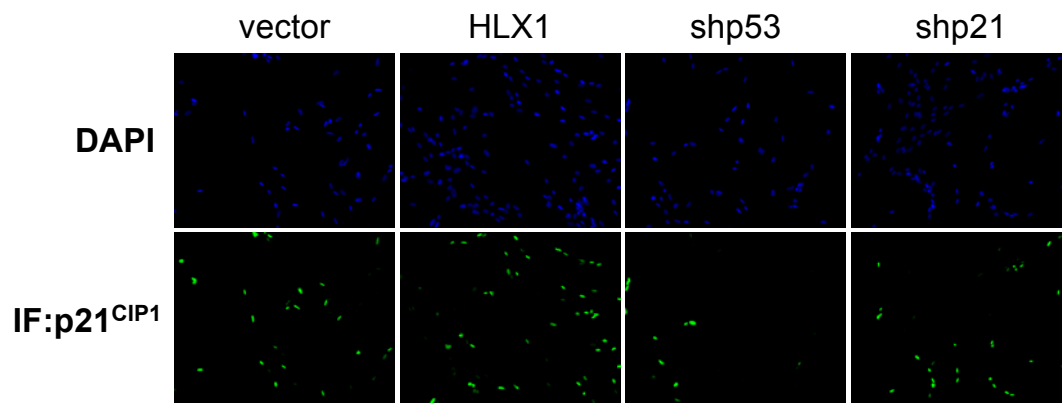
C



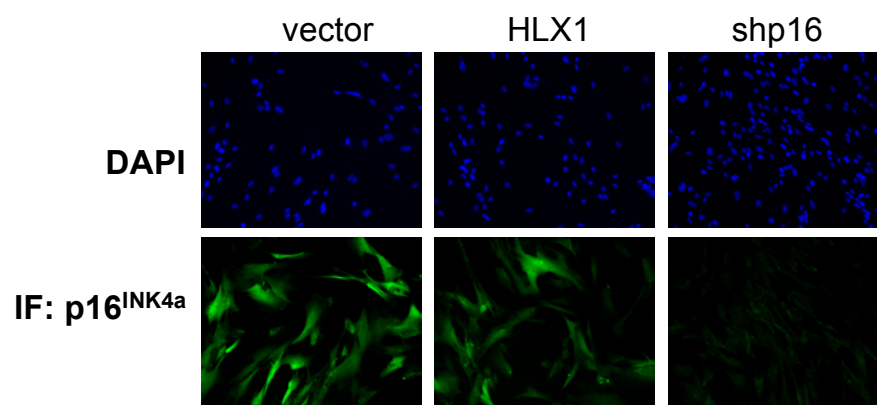
A

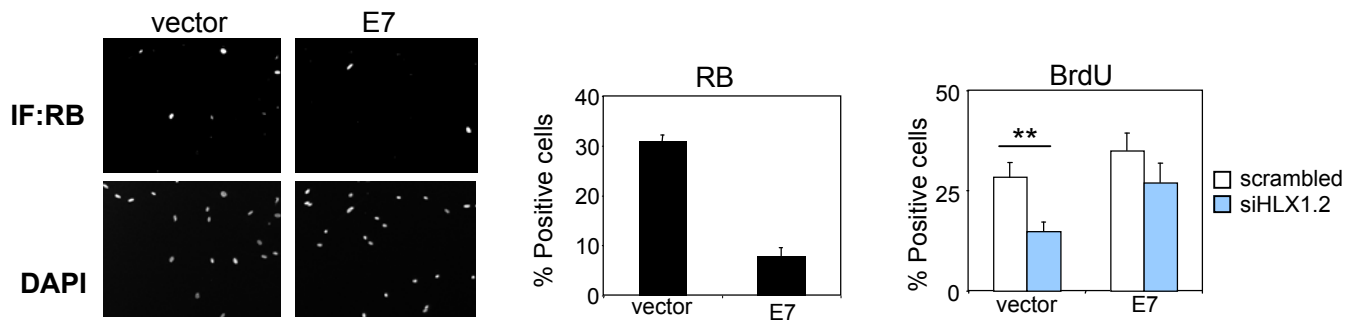


B

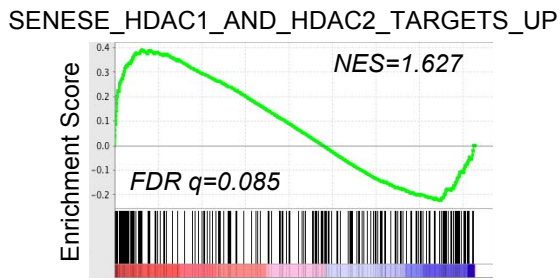


C

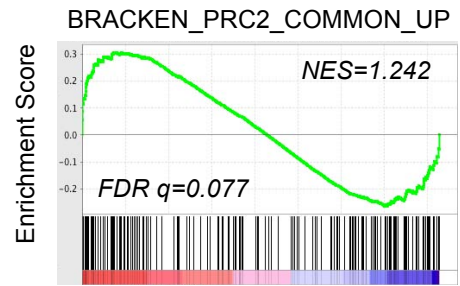




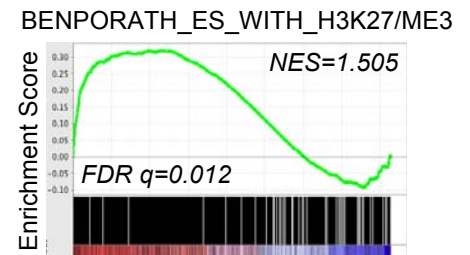
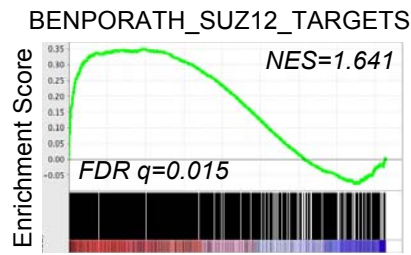
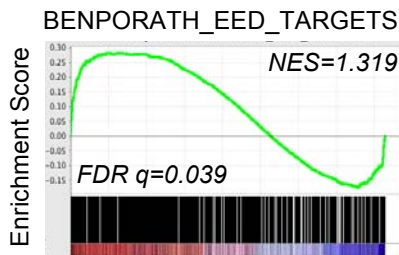
A



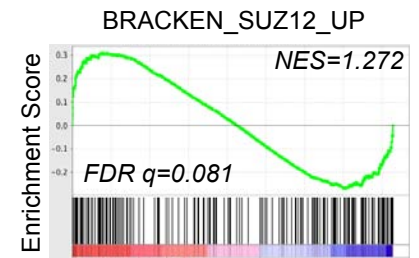
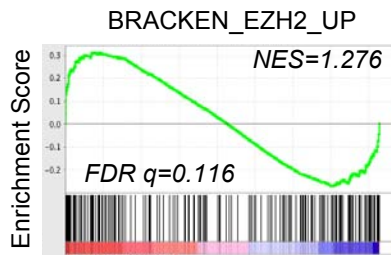
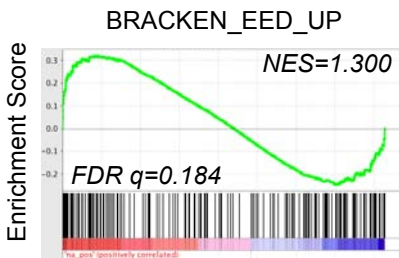
B



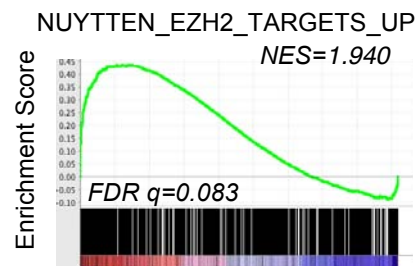
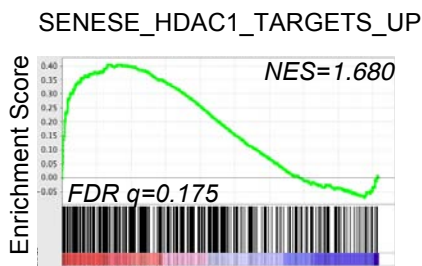
C



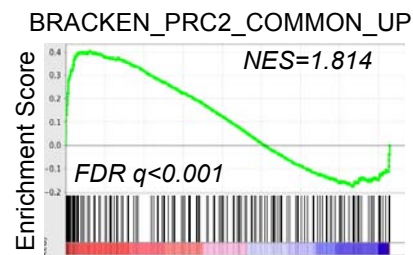
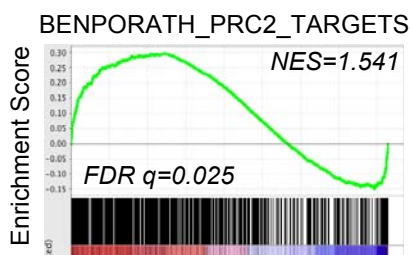
D



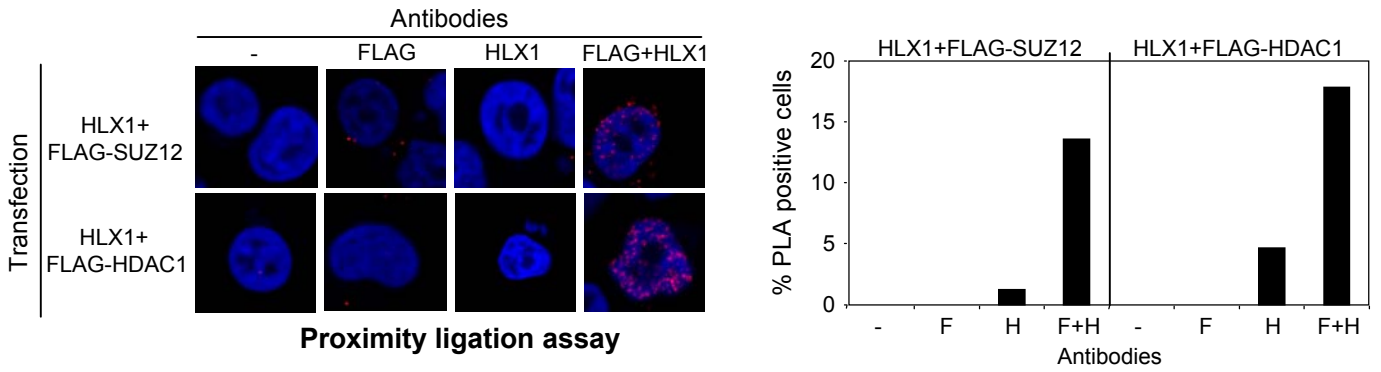
E



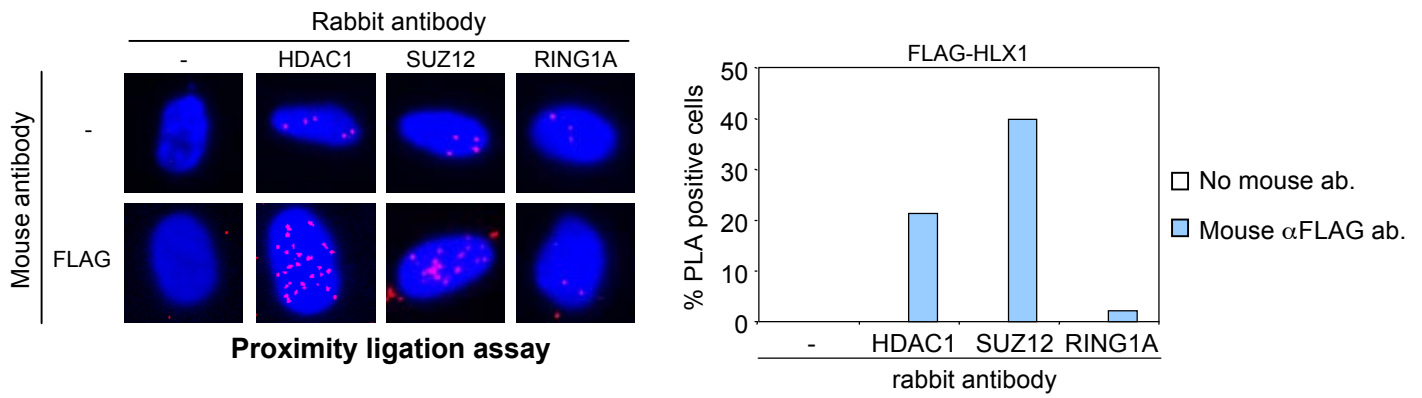
F



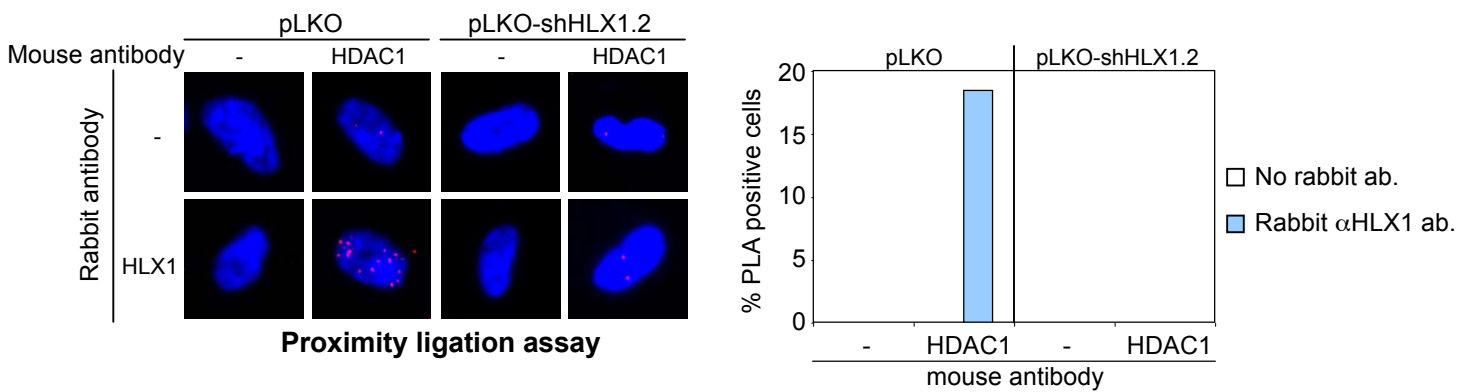
A

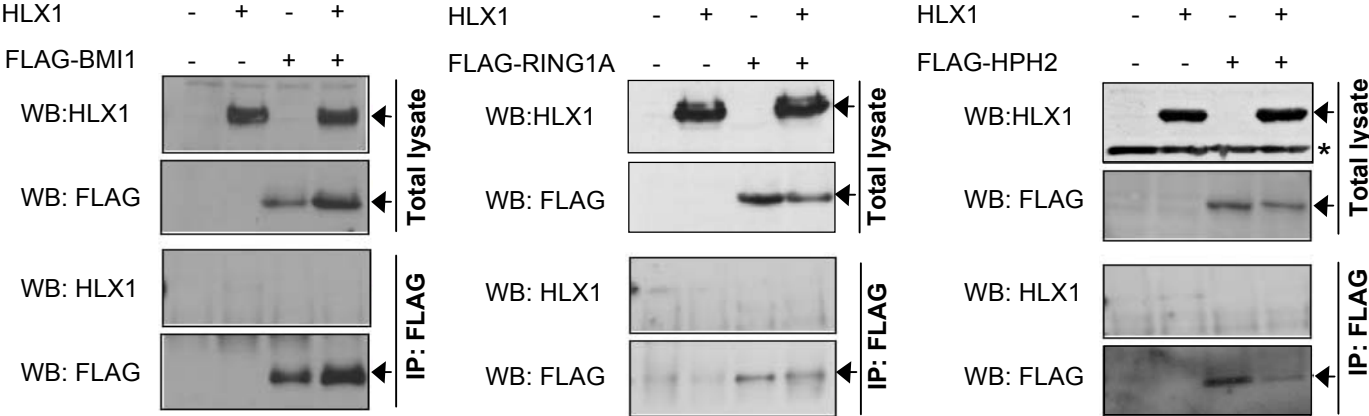


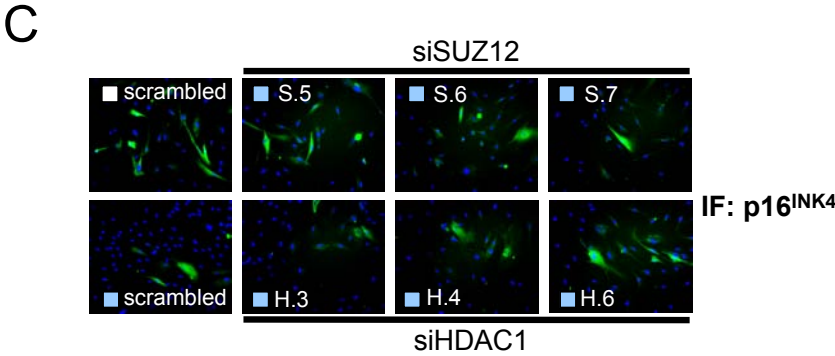
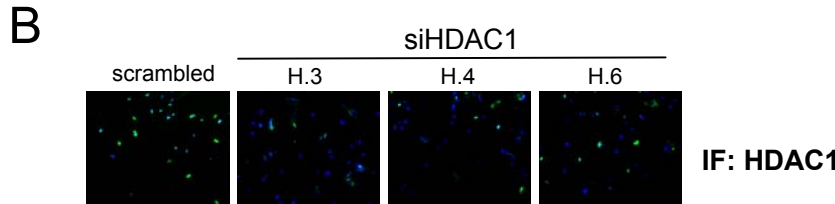
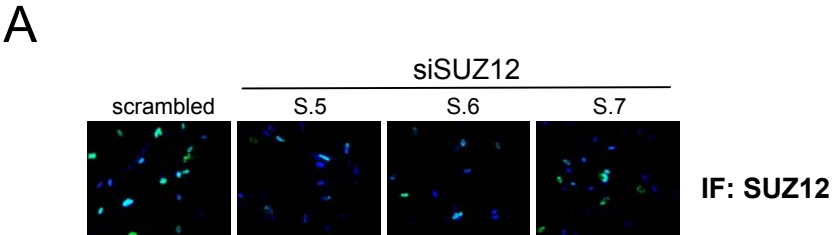
B



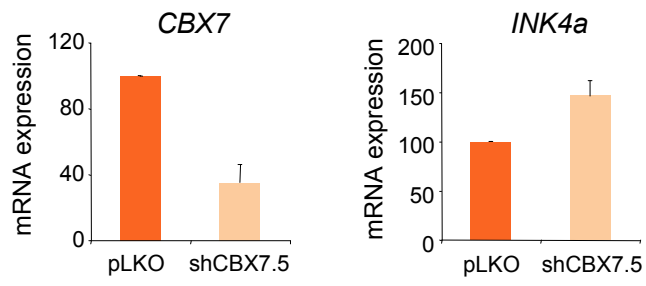
C



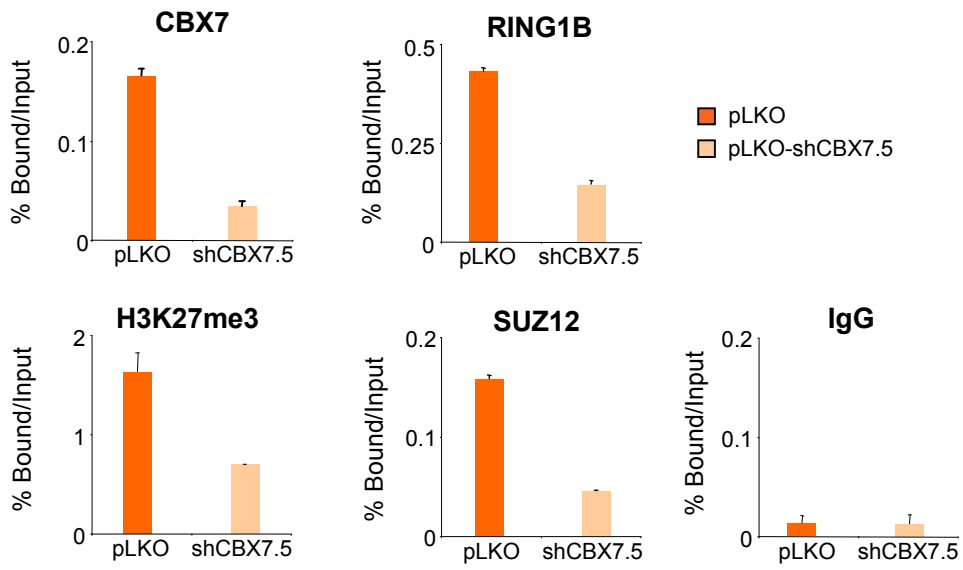


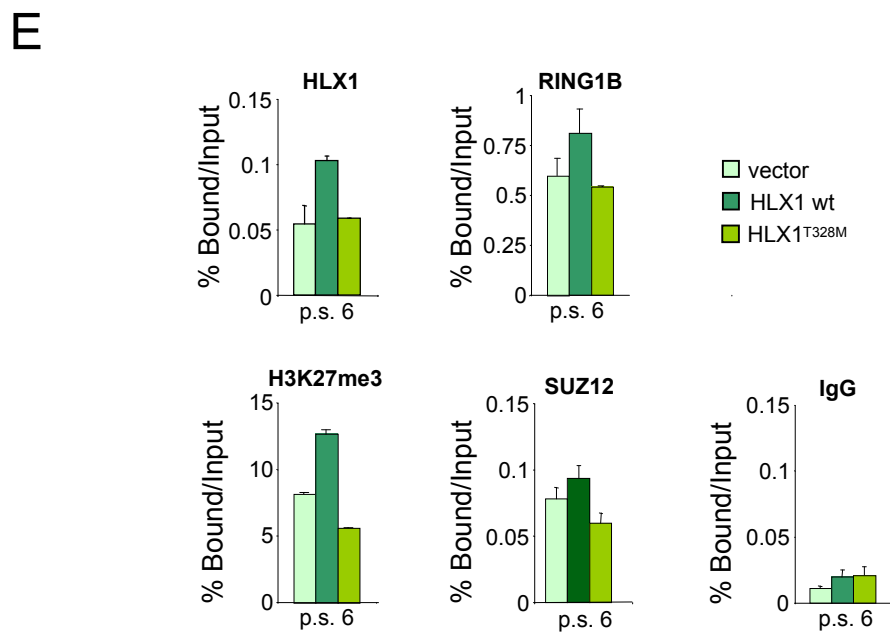
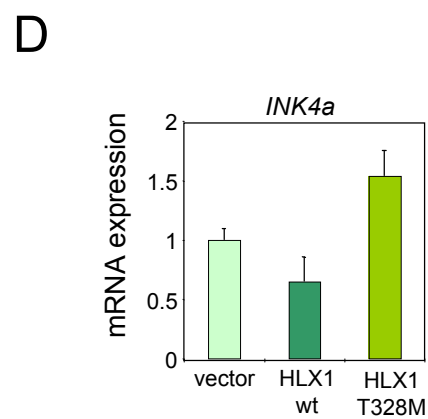
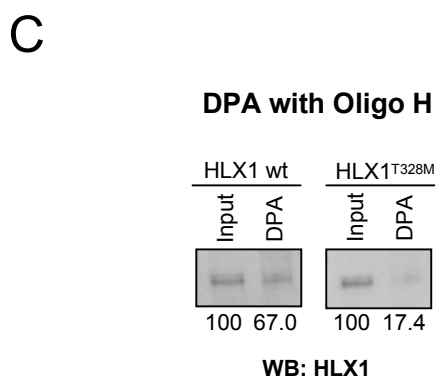
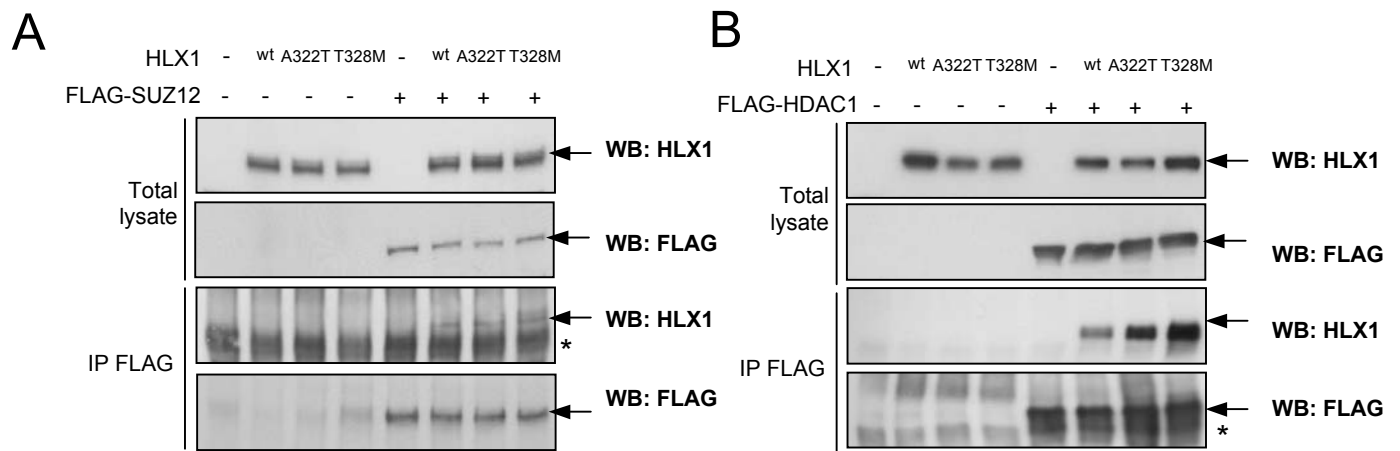


A

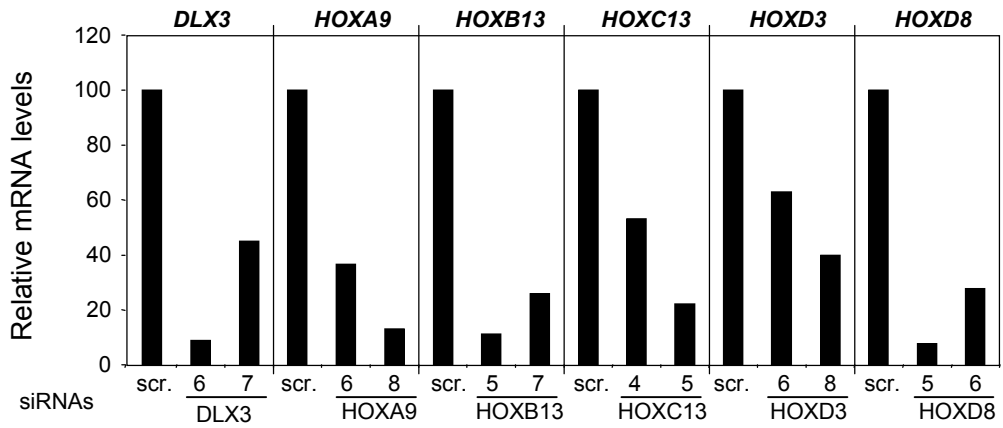


B

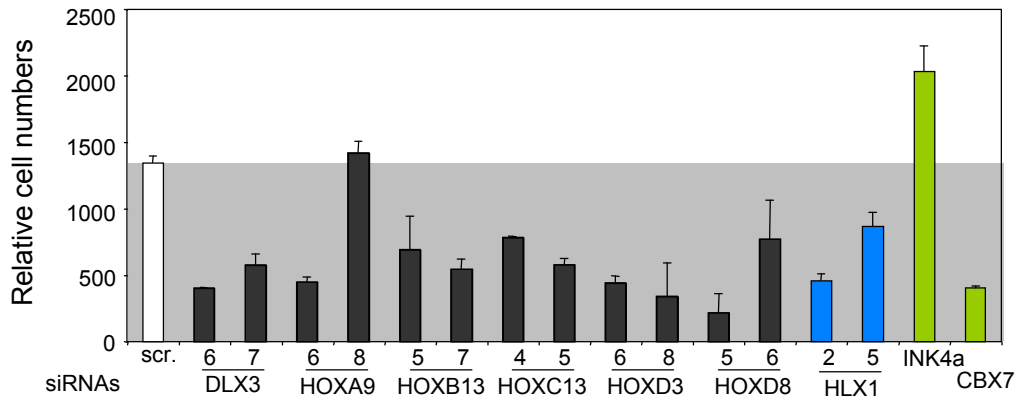




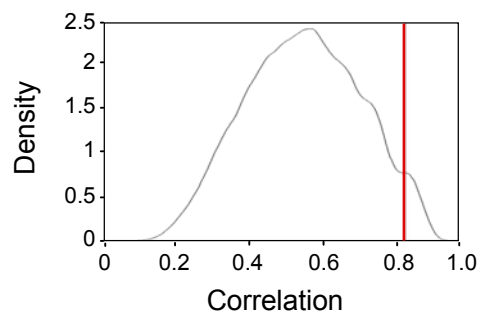
A



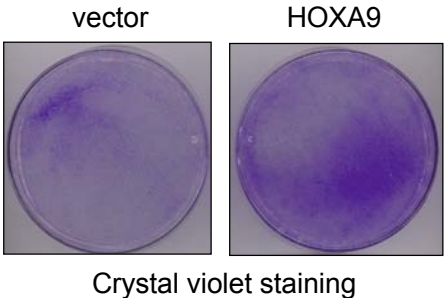
B



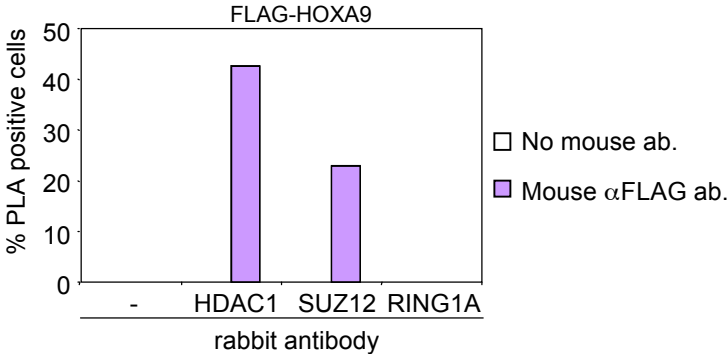
C



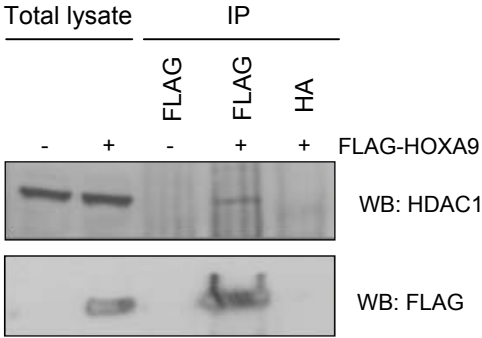
A



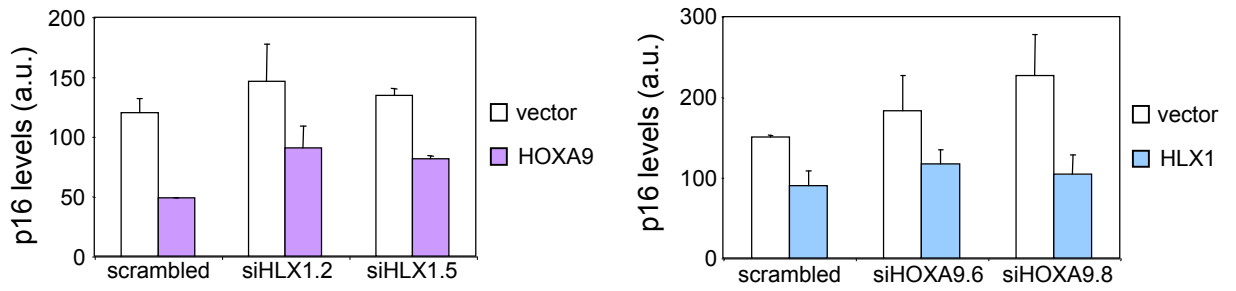
B



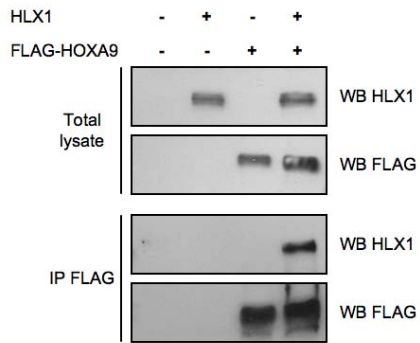
C



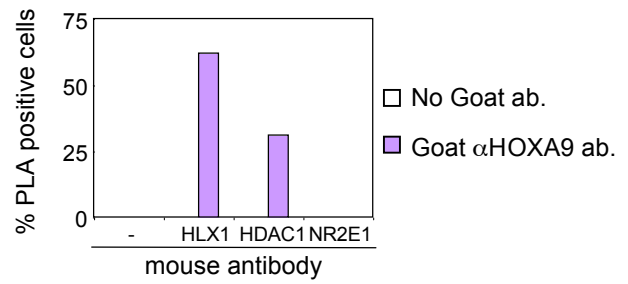
A



B

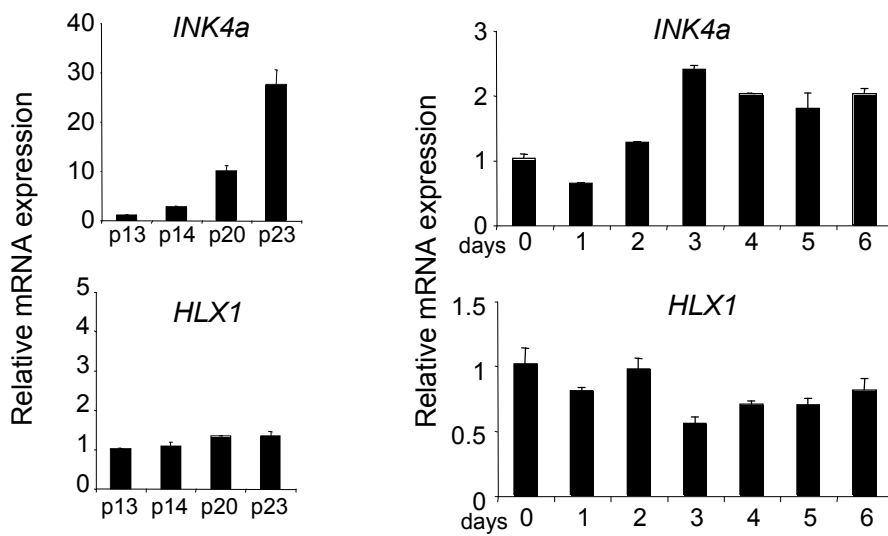


C

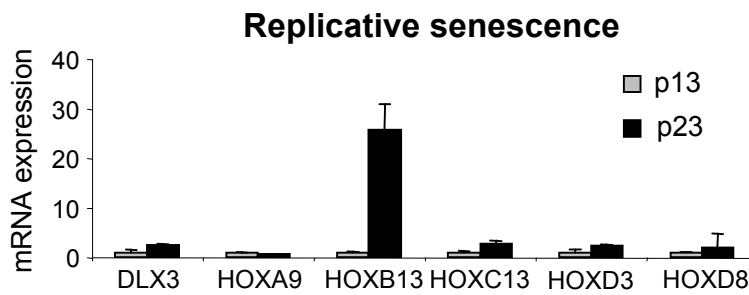


A

Replicative senescence Oncogene-induced senescence



B



C

Replicative senescence Oncogene-induced senescence

